Online ISSN 1848-3380, Print ISSN 0005-1144
ATKAFF 57(4), 1056–1069(2016)

*Dubravko Miljković*

# Active Noise Control in Light Aircraft Cabin Using Multichannel Coherent Method

DOI 10.7305/automatika.2017.12.1706
UDK [534.83:629.73.043*5,670 kg]:681.534.015.7.015.42

**Original scientific paper**

The paper deals with active noise control system for the cabin of a light aircraft. Basic system uses coherent averaging method of the residual error signal to produce signal that drives secondary source. Advanced versions of this system use a-priori information about noise waveform and adaptation process begins with the assumed waveform (sinus signal of adequate amplitude, phase and frequency or even low pass filtered referent noise signal). After testing single-channel system, achieved noise suppression is verified with additional simulation considering measured acoustic characteristics of real aircraft cabin (characterized by impulse responses). System could be extended to multichannel version of type SIMO (Single Input Multiple Output) where the same tacho/referent signal after adequate delay (acoustic propagation of the noise signal through the cabin) drives eight single-channel systems connected with multiple gain-delay combinations to reduce crosstalk between individual channels.

**Key words:** Active noise control, coherent averaging, multichannel system, light aircraft.

**Aktivno smanjenje buke u kabini lakog zrakoplova višekanalnom koherentnom metodom.** Rad opisuje višekanalni sustav za aktivno smanjenje buke u lakom zrakoplovu. Osnovni sustav se temelji na koherentnom usrednjavanju rezidualnog signala greške kojim se protufazno pogoni sekundarni izvor. Naprednije verzije ovog sustava koriste a-priori informaciju o valnom obliku buke te postupak adaptacije već započinje od pretpostavljenog valnog oblika (sinusoidalnog valnog oblika prikladne amplitude, faze i frekvencije ili čak samog niskim propustom filtriranog signala buke). Nakon ispitivanja jednokanalnog sustava, postignuta smanjenja buke su verificirana dodatnom simulacijom uzevši u obzir akustička svojstva kabine (pomoći impulsnih odziva). Sustav je proširiv na višekanalni tipa SIMO (Single Input Multiple Output), pri čemu se koristi isti taho/referentni signal koji se uz adekvatna kašnjenja (zbog akustičke propagacije buke u kabini) raspoređuje na osam jednokanalnih sustava povezanih višestrukim kombinacijama elemenata pojačanje-kašnjenje za smanjenje preslušavanja kanala.

**Ključne riječi:** Aktivno smanjenje buke, koherento usrednjavanje, višekanalni sustav, laki zrakoplov.

## 1 INTRODUCTION

The cabin interior of piston engine general aviation aircrafts is inherently noisy, [1-5]. High level of noise is not only annoying, tiring, increases stress and anxiety levels, poses a hearing risk but also considerably downgrades the quality of speech communication, that may reflect to a flight safety, [1,4-6]. Traditional way of dealing with high noise levels is application of passive methods for noise reduction, [1,8]. However, passive methods are generally inefficient and bulky at low frequencies where majority of noise sound energy is concentrated. Active methods are suitable for the reduction of low frequency noise, particularly if efforts are targeted towards achieving smaller zones of silence around pilot and passenger heads and ears. Active noise control (ANC) is reduction of unwanted noise by generating an acoustic signal that interferes with the noise, [1, 8-10]. The method for active noise control that uses coherent averaging of residual noise signal is presented, [1]. It is suitable for reduction of periodic noise commonly present in a cabin of light aircraft powered by the piston or turboprop engine.

## 2 SOURCES OF AIRCRAFT NOISE

Aircraft noise contains the following main components: engine noise, propeller noise, airframe noise and structure borne noise, [1,4,5]. Aircraft interior noise is the combination of all mentioned components that, with various degrees, penetrate into the aircraft cabin.

### 2.1 Engine noise

There exist various types of aircraft engines. The main types are piston, turboprop, turbojet, and turbofan. Engine noise is highly dependent on propulsion type. Most

common engine in light aircrafts is a piston engine. Piston engine noise is the result of pressure pulses on intake and exhaust during engine four cycles. In the case of piston engine, noise spectrum is dependent on the rotational speed, $N_{RPM}$, and number of cylinders. Cylinder firing rate, $f_{CFR}$, is dependent on the rotational speed and for a 4-cycle engines is given by (1), [1]:

$$f_{CFR} = \frac{N_{RPM}}{120} \tag{1}$$

Engine firing rate, $f_{EFR}$ is dependent on the $f_{CFR}$ and the number of cylinders ($N_C$), (2):

$$f_{EFR} = N_C f_{CFR} \tag{2}$$

Noise levels (SPL) produced by an engine are approximately determined by (3) where $B$ is cylinder bore (diameter), related to cylinder capacity $V \approx B^3$, [11]:

$$P = 10n\log_{10}(N_{RPM}) + 50\log_{10}(B) + const \tag{3}$$

### 2.2 Propeller noise

Propeller noise is composed of tonal and broadband components. Tonal component contains basic frequency and harmonics. The basic frequency $f_1$ or $f_{BPF}$ (blade pass frequency) is the product of the propeller rotation speed and the number of propeller blades, (4), [1]:

$$f_1 = f_{BPF} = \frac{N_{RPM} N_B}{60} \tag{4}$$

where is:

- $f_1$, $f_{BPF}$ basic frequency of tonal propeller component
- $N_{RPM}$ propeller rotation speed (rotations per minute)
- $N_B$ number of propeller blades

Besides base frequency harmonic components also appear, (5):

$$f_N = f_1 N \tag{5}$$

where is:

- $f_n$ frequency of $n$-th harmonic
- $N$ number of particular harmonic

Noise levels (SPL) produced by the propeller is defined by (6):

$$P = 10\log_{10}Q + 20\log_{10}P + 60 + K \tag{6}$$

where $Q$ is the air flow in m$^3$/s, $P$ is the static air pressure and $K$ is frequency dependent correction factor that can be found in tables, [12].

In a single engine aircraft propeller noise enters the cabin through the front window in the form of pressure pulses. The main propeller disturbance is radiated outside aircraft in the open space. With multiengine aircrafts propeller noise is more pronounced because the pilot and passengers are often in line with the propeller blades.

### 2.3 Airframe noise

Airframe noise is the result of air flow around the airframe. It is of the broadband flow mixing type except where a resonant cavity is formed (e.g. at control surface gaps). Its main characteristic is a great dependence on aircraft speed. Noise intensity is related to aircraft speed in the following equation, (7), [13]:

$$I = kv^n \tag{7}$$

where $v$ is the speed of an aircraft and the exponent $n$ varies between 5 and 6 and is dependent on the shape of fuselage. Considering relation between sound pressure level and sound intensity in (8) and assuming the round constant Z=400 Ns/m$^3$ for the specific acoustic impedance of the air

$$P = \sqrt{IZ} = 20\sqrt{I} \tag{8}$$

noise level is given by (9):

$$P \approx 20\sqrt{\alpha}Q \tag{9}$$

### 2.4 Structure borne noise

Structure borne noise results from the airframe vibrations. Various vibration modes excite structural modes. Acoustic space again has its acoustic modes that are excited by structural modes. This noise is quite complex and difficult to suppress, hence the best method is to prevent vibration entering the cabin.

### 2.5 Interior noise levels

Interior noise levels depend on the aircraft, but average values are 80 dB and above, up to 110 dB in case of some piston and turboprop aircrafts during takeoff and initial climb. Aircraft interior noise is also position dependent, ie. noise level and spectrum change a little through a cabin (there may exist small spots with a difference in the noise level of about 10 dB from average). Interior noise is generated predominantly by the engine, its exhaust, propeller and slipstream. Engine and propeller noise are of periodic type, and slipstream noise is a broadband noise. Noise levels in a cabin of Cessna 172 aircraft are shown in Table 1, [5].

## 3 TRADITIONAL METHODS FOR ACTIVE NOISE CONTROL INTRODUCTION

Most common methods for active noise control, [10], are feedforward method that can be broadband feedforward (Fig. 1) or narrowband feedforward such as synchronized waveform generator (Fig. 2), [10], and feedback method (Fig. 3). Each one uses some sort of adaptation algorithm like LMS, FX-LMS and variants for adapting a digital (usually FIR) filter. Diagrams are simplified and don't include influences of a secondary path. All these methods yield good results in cancellation of noise, but use of

*Table 1. Flight phases and corresponding noise levels*

| Phase | Noise level dBA (+/- 0.5dBA) |
|---|---|
| taxiing | 78.9 |
| hold | 80.2 |
| taxiing | 81.3 |
| take off run | 93.9 |
| take off | 91.1 |
| climb | 88.9 |
| cruise | 83.1 |
| descend | 74.0 |
| landing | 76.0 |

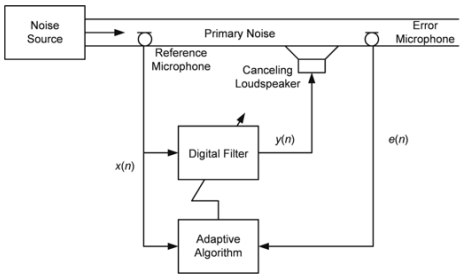


*Fig. 1. Broadband feedforward method.*

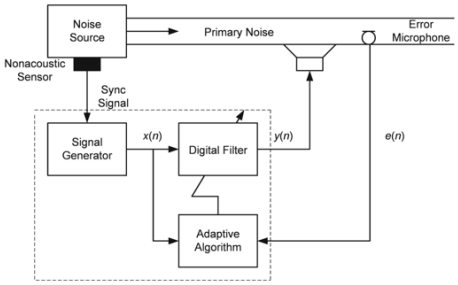


*Fig. 2. Narrowband feedforward method (synchronized waveform generator).*

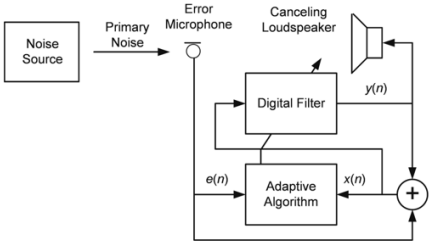


*Fig. 3. Feedback method.*

digital filter and LMS algorithm, [14], and variants, [10], makes them computationally intensive and almost always require specialized DSP hardware.

Large computational requirements come both from a long digital FIR filter and the LMS adaptation process, [14]. Adaptive FIR filter is illustrated in Fig. 4. Operation of the FIR filter is described by equation (10):

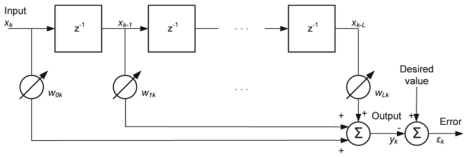


*Fig. 4. Adaptive FIR filter.*

$$y_k = \sum_{l=0}^{L} w_{lk} x_{k-l} \tag{10}$$

Error signal is determined as difference between the desired output and FIR filter output, (11), (12), (13) and (14):

$$\epsilon_k = d_k - y_k \tag{11}$$

$$\epsilon_k = d_k - X_k^T W_k \tag{12}$$

$$X_k = [x_k x_{k-1} \cdots x_{k-L}]^T \tag{13}$$

$$W_k = [w_{0k} w_{1k} \cdots w_{Lk}]^T \tag{14}$$

using the following convention:

- $X_k$ input signal in matrix (vector) form at the moment $k$
- $W_k$ weight factors in matrix (vector) form at the moment $k$
- $y_k$ desired value at the moment $k$
- $\epsilon_k$ error signal at the moment $k$
- $L$ digital filter length

Adaptation of filter weights by the LMS algorithm in matrix notation using a gradient estimate, [14], is given by (15) and (16):

$$W_{k+1} = W_k - \mu \hat{\nabla}_k \tag{15}$$

$$W_{k+1} = W_k + 2\mu\epsilon_k X_k \tag{16}$$

## 4 COHERENT AVERAGING OF SIGNALS

Coherent averaging is a digital technique for extracting the periodic signal from the noise, [15]. For averaging process to be successful three conditions must be fulfilled: signal waveform must be repetitive, noise must be random and uncorrelated with signal and temporal positions of each waveform period must be precisely known. When acoustic noise is of periodic nature coherent averaging reveals the

periodic component that, with the opposite phase, can be used to drive the secondary canceling acoustic source. Averaging process can be implemented in two ways. It can be arithmetic average of corresponding samples from successive periods. The other way is exponential averaging of corresponding samples. This method emphasizes recent changes in averaged signal and is more suitable for tracking dynamic changes. Input signal $f(t)$ has deterministic signal component $S(t)$ and noise signal component $N(t)$, (17):

$$f(t) = S(t) + N(t) \tag{17}$$

Let $f(t)$ be sampled every $T$ seconds. Value of each sample in an instant of period ($i = 1, 2, \ldots, n$) is the sum of deterministic signal component and noise signal component, (18):

$$f(iT) = S(iT) + N(iT)\,. \tag{18}$$

### 4.1 Arithmetic averaging

Coherent averaging process with arithmetic averaging is described in following equations. Every sample is stored in the register (memory). Value stored in the register after $m$ repetitions is, (19):

$$\sum_{k=1}^{m} f(iT) = \sum_{k=1}^{m} S(iT) + \sum_{k=1}^{m} N(iT) \tag{19}$$

Example of averaging 100 successive periods of a signal with the period of $L$ samples, is given in (20), (21) and (22):

$$x_1(1), x_1(2), x_1(3), \cdots, x_1(L), \tag{20}$$
$$x_2(1), x_2(2), x_2(3), \cdots, x_2(L), \tag{21}$$
$$\vdots$$
$$x_{100}(1), x_{100}(2), x_{100}(3), \cdots, x_{100}(L). \tag{22}$$

Averaging is performed on whole successive periods in such a way that corresponding samples from successive periods are averaged (all first samples from all periods, all second samples from all periods, etc.). This process is repeated for all samples from a period. Averaged waveform samples (waveform in an example has period of $L$ samples, averaged over 100 successive periods) are given in (23), (24) and (25):

$$\widehat{x}(1) = \frac{1}{100}\sum_{i=1}^{100} x_i(1), \tag{23}$$

$$\widehat{x}(2) = \frac{1}{100}\sum_{i=1}^{100} x_i(2), \tag{24}$$

$$\vdots$$

$$\widehat{x}(L) = \frac{1}{100}\sum_{i=1}^{100} x_i(L). \tag{25}$$

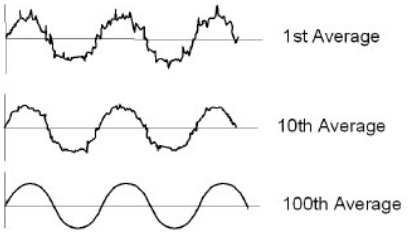


*Fig. 5. Noise reduction during coherent averaging process.*

Progression of the waveform noise reduction during coherent averaging process is shown in Fig. 5. Initial waveform is quite noisy, second waveform after ten averagings shows considerably less noise and after hundred averagings third waveform is almost a clear periodic signal. Signal component for sample at point $i$ is the same for every repetition if periodic signal is stationary and signal periods are correctly aligned in time, (26).

$$\sum_{k=1}^{m} S(iT) = mS(iT) \tag{26}$$

The assumption is that signal and noise are uncorrelated and that noise is random with average value equal to zero. After large number of repetitions, $N(iT)$ has effective (*RMS*) value $\sigma_n$, (27):

$$\sum_{k=1}^{m} N(iT) = \sqrt{m\sigma_n^2} = \sqrt{m}\sigma_n \tag{27}$$

Ratio between (26) and (27) gives signal-to-noise ratio ($SNR_m$) improvement after the $m$ repetitions, (28):

$$SNR_m = \frac{mS(iT)}{\sqrt{m}\sigma_n} = \sqrt{m}SNR \tag{28}$$

### 4.2 Exponential averaging

Another method for coherent averaging employs exponential averaging. Corresponding samples are averaged according to (29) and relation (30).

$$y_k = (1-\alpha)y_{k-1} + \alpha x_k \tag{29}$$

$$0 < \alpha < 1 \tag{30}$$

New sample is averaged with the previously averaged stored in memory. Using previous notation from arithmetic averaging to exponential averaging of corresponding samples follows (example of signal with period of $L$ samples), (31), (32) and (33):

$$\hat{x}_k(1) = (1-\alpha)\hat{x}_{k-1}(1) + \alpha x_k(1), \tag{31}$$
$$\hat{x}_k(2) = (1-\alpha)\hat{x}_{k-1}(2) + \alpha x_k(2), \tag{32}$$
$$\vdots$$
$$\hat{x}_k(L) = (1-\alpha)\hat{x}_{k-1}(L) + \alpha x_k(L). \tag{33}$$

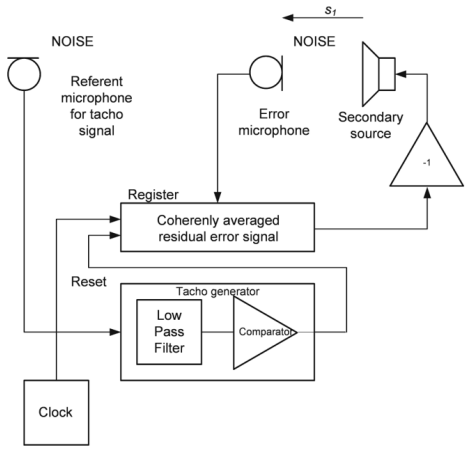


*Fig. 6. Block diagram of the single channel system.*

Time constant of the exponential averaging $\tau$ depends on the value of $\alpha$, (34):

$$\tau = \frac{2}{\alpha} - 1 \tag{34}$$

In real use the value of the coefficient $\alpha$ is around $0.1 - 0.02$, depending on desired dynamic properties of the algorithm (how fast algorithm tracks changes in acoustic noise signal) and convergence properties. As can be seen, new samples cause a little change to the current average of samples, but after $\tau$ periods new samples will overtake previous history stored in $y_{k-1}$.

## 5 COHERENT AVERAGING METHOD FOR THE ACTIVE NOISE CONTROL

### 5.1 System overview

Block diagram of the system is shown in Fig. 6, [1]. It consists of a clock, tacho generator, register for coherent averaging, amplifier with phase reversal and two microphones (referent and error). Clock signal supplies sample rate to the register for the operation of the whole system including A/D and D/A conversion (for clarity A/D and D/A converters are not shown in a figure).

### 5.2 Tacho signal

Beginning of each period is determined from the tacho signal (eg. inductive or optical sensor). In this case there is no need for referent microphone. If this type of tacho signal is not available, it can be extracted from original acoustic noise picked by the referent microphone. Block diagram of such tacho generator is given in Fig. 7. Signal from the microphone passes through the low pass filter to remove higher frequency components that would cause spurious zero crossings when detecting basic period of the periodic

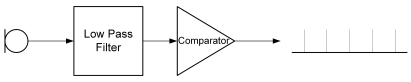


*Fig. 7. Block diagram of tacho generator.*

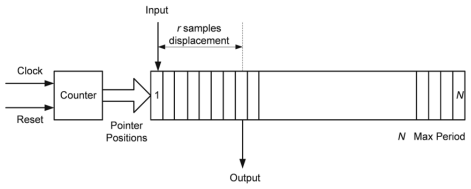


*Fig. 8. Block diagram of register.*

noise signal. Zero crossing detection is performed by a comparator that has small hysteresis. Output from comparator is the tacho signal (trigger) necessary for coherent averaging of periods of residual noise signal.

### 5.3 Register

The register (Fig. 8) consists of numerous words (memory locations containing number of bits corresponding to A/D and D/A converter in use) that can store waveform of the maximal period length of the signal for secondary source. The register has a pointer that points to the word that is addressed. This pointer can be reset by the tacho signal, so with the beginning of each new period pointer always points to the first word in the register. There is also branch output from the register word separated by the specific number of samples to accommodate for the acoustic signal propagation between the secondary source and error microphone. In this way with every new clock signal, one word enters the register and one, separated by the fixed number of words is picked out from the register. Updated word that enters the register is exponentially averaged present content of the word with the new residual error sample.

### 5.4 Description of the system operation

For easier understanding of the operation of the system it will be assumed that properties of acoustic noise signal are not changing (condition that is not required, here it is just for simplification). When system starts with the operation, the register content is empty with all words containing zeros and there is no signal at secondary source, hence there is no cancellation of acoustic noise. All present noise is picked as residual noise by error microphone and samples of this error signal are exponentially averaged with empty values in the register. After the first period the register is not empty any more but contains (although with small amplitude and envelope) replica of the noise signal. This signal now drives the secondary source and causes small can-

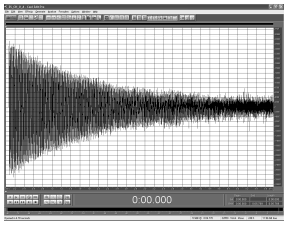


*Fig. 9. Residual error source signal (*0.2 *s/div).*

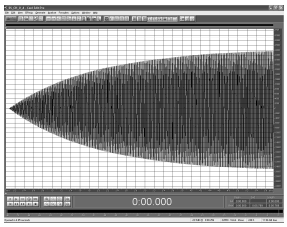


*Fig. 10. Secondary signal (*0.2 *s/div).*

cellation of the acoustic noise. Now there is again residual error signal, but this time slightly lower than in the previous period that is again averaged with corresponding samples of waveform stored in registry. Little by little, after successive coherent averagings, the operation reaches equilibrium and the waveform stored in the register closely resembles the acoustic noise signal both in the waveform and amplitude. Progress of residual error minimization and development of the canceling signal for the secondary source during the convergence of an algorithm is shown in Fig. 9, 10, 11 and 12. Convergence is achieved within few seconds. In Fig. 9 one can see that residual noise error decreases while the signal of secondary source, Fig. 10, increases until it stabilizes. Value of improvement of signal-to-noise ratio in coherent averaging process, (28), equals to maximal achievable value of noise cancellation. This value can only be achieved with perfectly stationary periodic signal with additive noise. Small fluctuations between period lengths and amplitude variation of periodic component will somewhat decrease this value.

### 5.5 Influence of the secondary path

The secondary path response includes frequency and phase response of the loudspeaker and microphone. Frequency responses of a microphone and a loudspeaker are generally flat (within few dB in a frequency range of interest) and their influence to the convergence is negligible (waveform generator will adapt to a slightly different amplitude of a signal). The main problem is phase shift in the loudspeaker. This phase shift is frequency dependent and hinder accurate alignment of output and error signal during averaging. Phase response of the microphone is illustrated in Fig. 13, and of the loudspeaker in Fig. 14. Phase

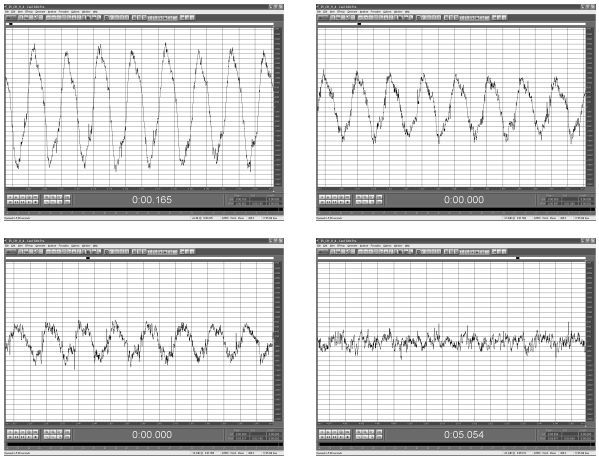


*Fig. 11. a-d. Progression of the residual error signal waveform during convergence (*0.05 *s/div).*

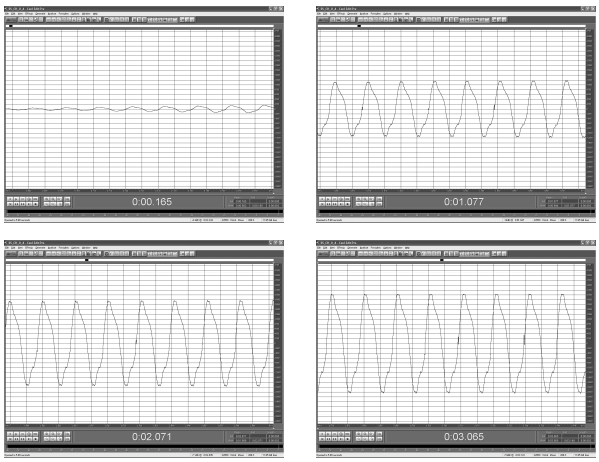


*Fig. 12. a-d. Progression of the secondary source signal waveform during convergence (*0.05 *s/div).*

response of the microphone is quite flat across large frequency range, however loudspeaker doesn't have that flat response. Reasonably flat and slowly changing phase (no sudden 180° changes) characteristics is common, however in some cases phase correction may be necessary (simple passive solution may suffice).

### 5.6 Calibration of sound signal propagation times

There is a fixed time interval $T$ for noise signal to propagate acoustically across the distance $s$ from the secondary source to the error microphone that must be considered, (35):

$$T = \frac{s}{v} \tag{35}$$

where $v$ is speed of sound in the air, (36):

$$v = 331,5 + 0,6t \tag{36}$$

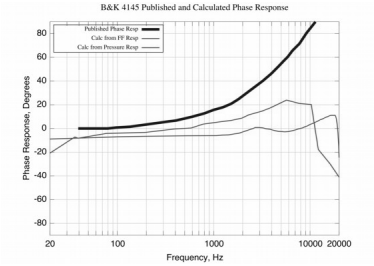


*Fig. 13. Example: phase response of the microphone.*

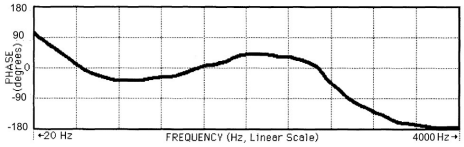


*Fig. 14. Example: phase response of the loudspeaker.*

where $t$ is air temperature in °C.

Number of samples $N$ during this period is determined by (37):

$$N = f_s T \tag{37}$$

where $f_s$ is a signal sampling rate.

Distance and sound propagation delay in samples for $f_s = 22050$ Hz are shown in Table 2 and in more detail later in Fig. 21.

This time interval little changes (almost constant) and is determined by the calibration process before the use of the noise cancellation system. Calibration is performed by the pilot tone and measurement of the phase change between source and microphone using the crosscorrelation of these two signals. It was already mentioned that sound propagation time between the loudspeaker and the microphone must be considered and determined. Due to phase characteristics of the secondary source it is also necessary to consider additional small time shift for correction due to the phase shift $\theta_P$ and group delay of the secondary source at the frequency of the calibration tone. Calibration process is performed before the first use by generating short sinusoidal pilot tone at the frequency of most interest $f_P$ (presumably $f_1$ – blade pass frequency in cruise) and is based on correlation function between signal of the generated pilot tone $x_1$ and signal picked from the from microphone during calibration, $x_2$. Correlation values are calculated for time shifts in samples $\tau_\Delta$, (38) using floor and ceiling function, distance $d$ (with 25% tolerance), speed of sound $v$, sample frequency $f_s$, pilot tone frequency $f_P$ and maximal 90° phase shift). The largest correlation value with corresponding $\tau_\Delta$ is determined according to (38) and (39):

*Table 2. Distance and sound propagation delay expressed in number of samples*

| Distance | front seats | | rear seats | |
|---|---|---|---|---|
| | *in cm* | *in samples* | *in cm* | *in samples* |
| $s_1$ | 102 | 65 | 190 | 122 |
| $s_2$ | 20 | 13 | 20 | 13 |

$$r_{12}(\tau_\Delta) = \frac{1}{N-\tau_\Delta}\sum_{n=\tau_\Delta}^{N} x_1(n)x_2(n-\tau_\Delta)$$

$$\tau_\Delta = \left[0.75\frac{df_s}{v} - \frac{90f_s}{360f_p}\right], ..., \left[1.25\frac{df_s}{v} - \frac{90f_s}{360f_p}\right] \tag{38}$$

$$r = \arg\min_{\tau_\Delta}(r_{12}(\tau_\Delta)) \tag{39}$$

where $r$ is the time shift represented in a number of samples for which highest correlation value between two signals $r_{12}$(m) is determined. Value of $r$ includes total sound delay in samples produced by the sound propagation through the air, as determined in (37), and phase characteristics of the loudspeaker. This is the number of samples that separates positions of pointers for input and output of registry.

### 5.7 Convergence properties

Convergence is dependent on the amplitude and phase response of the secondary path. It is assured for phase shifts, (40):

$$\theta \in [-90°, +90°] \tag{40}$$

Convergence speed is proportional to the product in (41):

$$\alpha\cos(\theta) \tag{41}$$

The higher the $\alpha$ and the lower the phase shift $\theta$ within the secondary path, the faster will be the convergence. When the phase shift approaches 90° convergence is becoming very slow. If phase shift $\theta$ is outside this interval the algorithm will not converge but diverge. Frequency shift in the secondary path for each and every frequency component used for noise cancellation in the secondary source must be within the previous interval for the system to converge. Higher frequencies with a phase shift outside the interval can be eliminated by low-pass cut-off (usually switch capacitor) filter following the D/A converter. In this way possible rare frequency components that do not fit in ±90° phase interval will be eliminated by low pass filter before A/D and after D/A. Such filters are parts of digital control systems with analog signals anyway.

### 5.8 Numerical complexity

The method is considerably numerically simpler than the FXLMS algorithm. In the FXLMS algorithms we have two

*Table 3. Numerical complexity (per new sample)*

| Algorithm | Additions | Multiplications |
|---|---|---|
| FXLMS | $S$+$W$+1 | $S$+$W$+2 |
| Synchronized averaging | 1 | 2 (1*) |

*If leakage factor (1-$\alpha$) from (29) is omitted

filters $W(z)$ and $S(z)$ of length $S$ and $W$, [10]. Typical filter lengths are at least 256 taps. Adaptation process in the FXLMS algorithm is described in (42).

$$w(n+1) = w(n) + \mu x'(n)e(n) \tag{42}$$

Secondary path estimation in the FXLMS algorithm is assumed to be off-line, otherwise numerical complexity of the FXLMS algorithm would be even greater. In synchronous averaging we have just one addition and two (*one) multiplications. Comparison is shown in Table 3. Even if one uses pointer offset by $r$ samples from (39), all operations with pointers can be implemented with three pointers, one zero comparison and no additional mathematical operations.

## 6 ADVANCED VERSIONS OF THE SYSTEM

Instead of starting convergence with the empty register it is possible to preload the register with approximation of the desired waveform, [1]. This way convergence will be a less tedious task.

### 6.1 Preloading the register with the sinusoidal signal with a frequency of a tacho signal

Instead of starting with the empty waveform in the register, it is loaded with a sinusoidal waveform corresponding to the frequency of the tacho signal and with amplitude corresponding to a referent noise signal, Fig. 15. During the convergence process starting sinusoidal waveform is transformed to a more appropriate waveform containing additional harmonics producing the signal that is suitable for driving the secondary source.

### 6.2 Preloading the register with the low pass filtered referent signal

This approach goes a step further and instead of the empty register, or sinusoidal approximation of the desired signal for driving secondary sources starts with low pass filtered reference noise signal that much closer reassembles (in opposite phase) the desired noise cancelling signal waveform, [1], Fig. 16, (concept, delayed signal may go to summation).

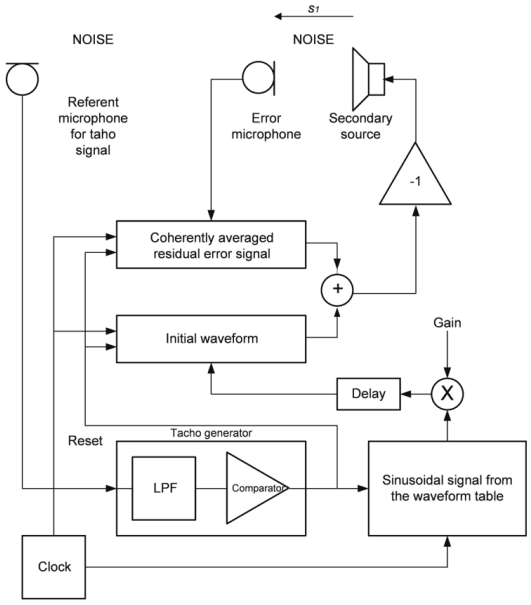


*Fig. 15. Block diagram of single channel system with preloading with the sinusoidal signal.*

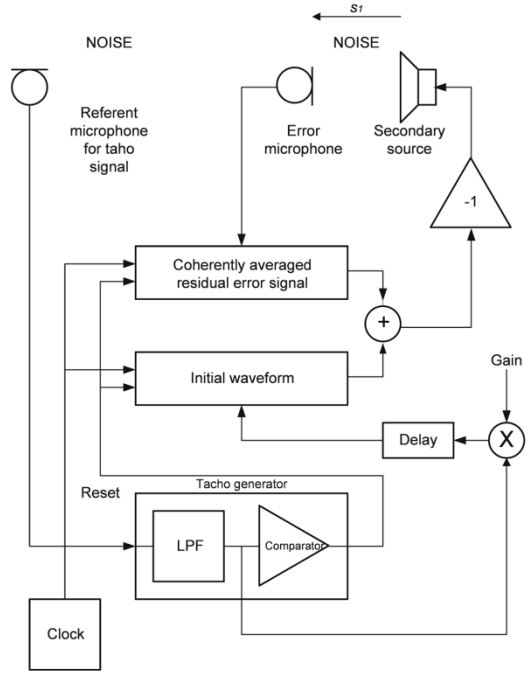


*Fig. 16. Block diagram of single channel system with preloading with the referent signal.*

## 7 POSITIONING OF MICROPHONES AND SECONDARY SOURCES

The Cessna 172 Skyhawk is a four-seat, single-engine, high-wing aircraft. It is the most successful mass produced

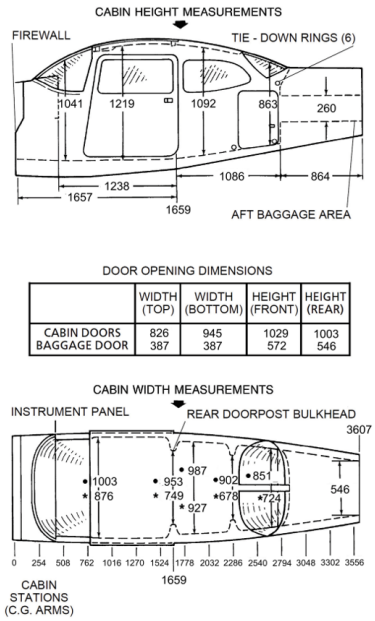


*Fig. 17. Cessna 172 – cabin dimensions.*

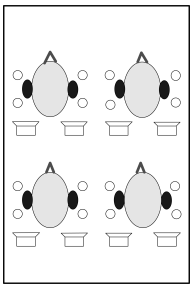

*Fig. 18. Layout in horizontal plane.*

light aircraft in history. The cabin with its dimensions is illustrated in Fig. 17, [16]. Layout of intended positions for microphones and secondary sources in horizontal plane is illustrated in Fig. 18 and in vertical plane in Fig 19. For each person there are two slightly displaced secondary sources above the head, one for each ear. Error microphones positioned behind in the headrest are necessary for ANC system operation. Measurement microphones in Fig. 18, are used for noise attenuation verifications and are not used in actual ANC system. Distance between windscreen, secondary sources, ears of passengers and measurement microphones positions are shown in Fig. 20.

Noise levels at the front seats are approx. 1.5 dB lower than at the very front position in the cabin (windshield) and 3 dB lower than at the rear seat positions.

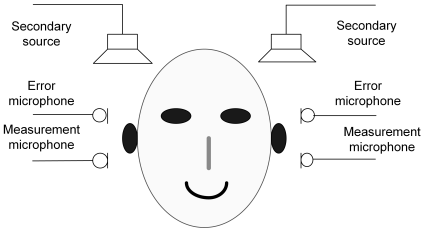


*Fig. 19. Layout in vertical plane.*

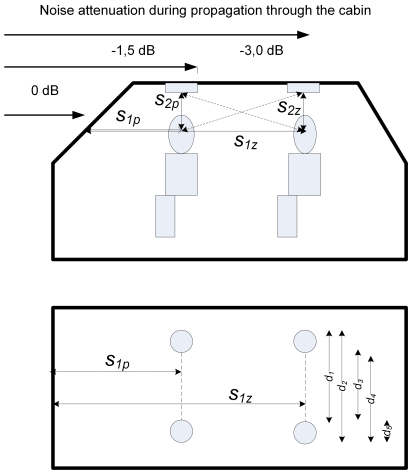


*Fig. 20. Distances between windscreen, secondary sources, ears of passengers and measurement microphones positions for direct paths and sound crossover.*

- $s_{1P}$ - distance between the windscreen and ears of front seat passengers
- $s_{1Z}$ - distance between the windscreen and ears of rear seat passengers
- $s_{2P}$ - distance between forward secondary sources and ears of front seat passengers
- $s_{2Z}$ - distance between rear secondary sources and ears of rear seat passengers
- $d_1$, $d_2$, $d_3$, $d_4$ and $d_5$ - lateral distances among ears of passengers

## 8 EXTENSION TO A MULTICHANNEL SYSTEM

The method employed in the single channel system may be extended to multiple channels considering the crossovers (delay and attenuation). In this way we get eight-channel system for four seat light aircraft that produces eight silent zones around ear positions of pilot and passengers. Crossover elements consist of attenuation and a delay, Fig. 21. Single channel system with crosstalk elements

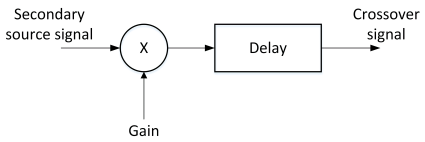


*Fig. 21. Crossover element.*

*Table 4. Typical crossover delays and attenuations (compared to level of secondary source for that seat)*

| Between | Delay (samples) at $f_s = 22050$ Hz | Attenuation dB (approx.) |
|---|---|---|
| two channels for the same seat | $\approx 30$ (head) | 5 |
| front seats | 46 | 6 |
| rear seats | 46 | 6 |
| front and rear seats | 60 | 8 |
| front and rear seats (diagonal) | 76 | 10 |

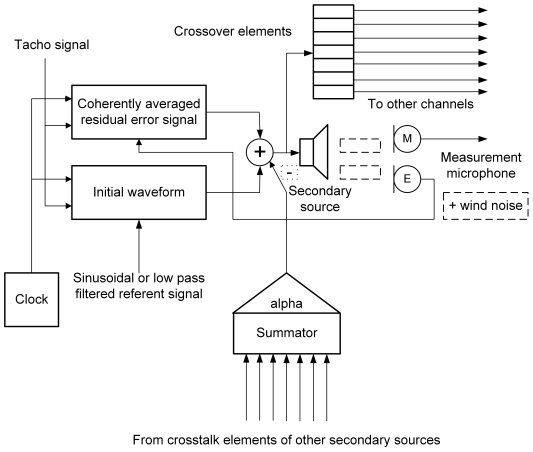


*Fig. 22. Single channel system with crosstalk elements.*

is shown in Fig. 22.

Approximate values for delays and attenuations are shown in Table 4.

Multichannel system with eight channels is shown in Fig. 23. All channels use the same tacho signal from common tacho signal generator.

Only direct paths from secondary sources are considered (in crossover elements), cabin reflections originating from secondary sources are omitted due to much lower contribution. This crosstalk somewhat distorts ideal resulting noise canceling waveform at the ear position produced by secondary source specifically positioned and dedicated for that ear. Introduction of crossover elements slightly improves convergence.

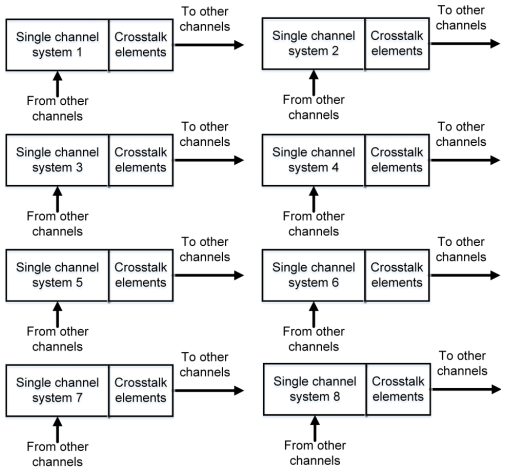


*Fig. 23. Multichannel system with eight channels.*

*Table 5. Test signals*

| Signal | RPM |
|---|---|
| C172_rpm1 | 1130 |
| C172_rpm2 | 1705 |
| C172_rpm3 | 1917 |
| C172_rpm4 | 2299 |
| tracking c172_rpm3 step to c172_rpm4 | step 1917 to 2299 |

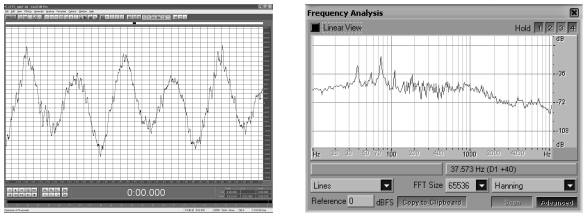


*Fig. 24. a-b. Signal c172_rpm1 (left, a). Spectrum (right, b).*

## 9 SIMULATION WITH REAL WORLD SIGNALS

Testing was performed with four recorded signals: C172_rpm1, C172_rpm2, C172_rpm3 and C172_rpm4 that correspond to various engine RPMs, Table 5. These signals were taken from quality recordings available in MS FS2004 flight simulator. Waveforms of test signals are shown in Figs. 24-27a (0.2 s/div) and corresponding spectra in Figs. 24-27b. Please note that with RPM change there is not just a simple shift in spectrum, but more complex change both in waveform and the spectrum.

In simulation attenuated noise signal is measured in three ways: unweighted signal, A-weighting and C-weighting. A-weighting is widely adopted for environmental noise measurement and C-weighting in aviation. Difference is less pronounced with A-weighting because

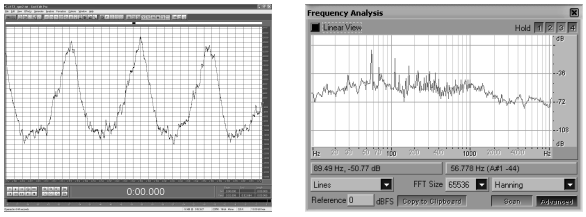


*Fig. 25. a-b. Signal c172_rpm2 (left, a). Spectrum (right, b).*

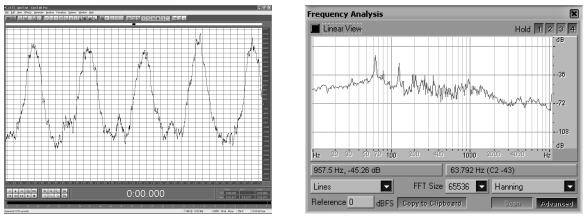


*Fig. 26. a-b. Signal c172_rpm3 (left, a). Spectrum (right, b).*

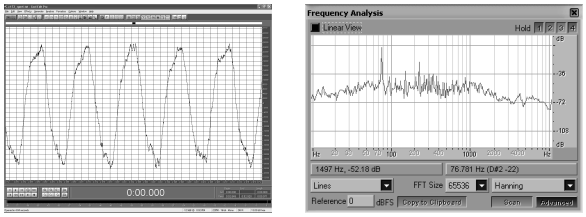


*Fig. 27. a-b. Signal c172_rpm4 (left, a). Spectrum (right, b).*

its weighting curve significantly diminishes contributions of low frequencies that are best canceled with active noise control systems. In this way considerable attenuations at low frequencies corresponding to engine and propeller noise are underrepresented in A-weighted results.

### 9.1 Basic system results

Results for the basic single channel system (i.e., one that does not use register preloading) are shown in in Fig. 28 (0.2 s/div) and Table 6.

### 9.2 Advanced system results with sinusoidal preloading

When the register is preloaded with the sinusoidal signal of the frequency of the tacho generator, system starts convergence process from a better position, hence convergence time is much shorter. Test signal (C172_rpm1), signal of the secondary source, spectral differences with ANC on-off and achieved ANR attenuation results are presented in Fig. 29 (0.2 s/div) and Table 7.

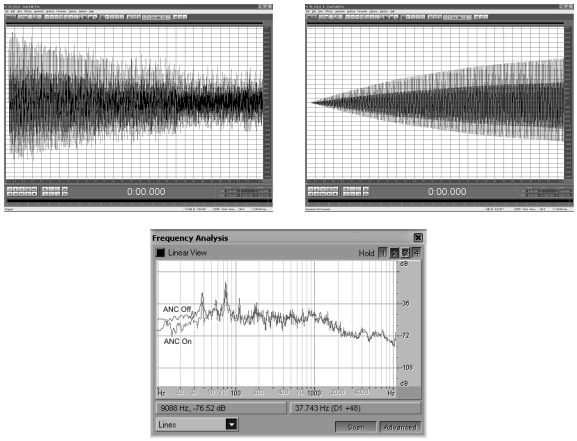


*Fig. 28. a-c. Error signal (top left, a). Secondary source (top right, b). Noise spectrum with ANC on/off (bottom, c).*

*Table 6. Noise attenuation for the basic system*

| Test signal | Difference with various weighting | | |
|---|---|---|---|
| | *unweigh.* | *A-weighting* | *C-weighting* |
| C172_rpm1 | 9,90 | 1,20 | 9,77 |
| C172_rpm2 | 13,26 | 1,76 | 12,81 |
| C172_rpm3 | 13,06 | 1,49 | 12,78 |
| C172_rpm4 | 21,42 | 6,10 | 21,21 |

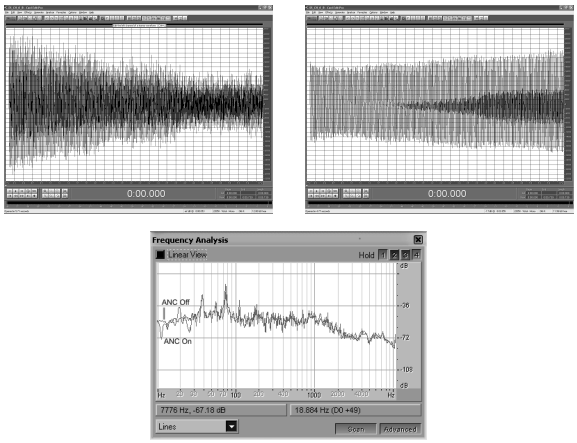


*Fig. 29. a-c. Error signal (top left, a). Secondary source (top right, b). Noise spectrum with ANC on/off (bottom, c).*

### 9.3 Advanced system results with referent signal preloading

When the register is preloaded with a low pass filtered reference signal, convergence time is much lower, for practical purpose almost instantaneous. Test signal (C172_rpm1), signal of the secondary source, spectral differences in noise reduction with ANC on/off and achieved ANR attenuation results are presented in Fig. 30 (0.2 s/div) and Table 8.

*Table 7. Noise attenuation for advanced system with sinusoidal preloading*

| Test signal | Attenuation with various weighting | | |
|---|---|---|---|
| | *unweigh.* | *A-weighting* | *C-weighting* |
| C172_rpm1 | 8,97 | 1,17 | 9,04 |
| C172_rpm2 | 14,22 | 1,63 | 13,67 |
| C172_rpm3 | 14,24 | 1,34 | 13,02 |
| C172_rpm4 | 20,94 | 5,99 | 20,78 |

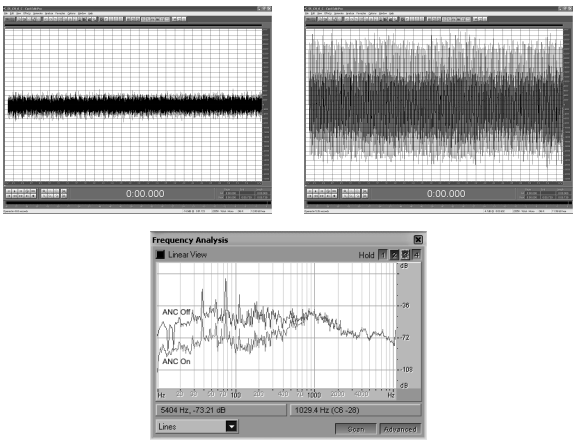


*Fig. 30. a-c. Error signal (top left, a). Secondary source (top right, b). Noise spectrum with ANC on/off (bottom, c).*

### 9.4 Dynamic properties

To investigate dynamic properties the test signal contained 3s of noise at 2000 RPM followed by an abrupt change (throttle advancement) to 2200 RPM (Fig. 31a). After the initial convergence, and the abrupt change in test signal three seconds later there was the second convergence. Due to the influence of echo and nonstationarity of the noise complete convergence was not achieved in either case (significant residual noise remains). Methods with sinusoidal, Fig. 31c and referent signal, Fig. 31d, as initial signal in coherent averaging process have better tracking properties than the basic system (but still good), Fig. 31b.

*Table 8. Noise attenuation for advanced system with referent signal preloading*

| Test signal | Attenuation with various weighting | | |
|---|---|---|---|
| | *unweigh.* | *A-weighting* | *C-weighting* |
| C172_rpm1 | 9,90 | 1,20 | 9,77 |
| C172_rpm2 | 13,26 | 1,76 | 12,81 |
| C172_rpm3 | 13,06 | 1,49 | 12,78 |
| C172_rpm4 | 21,42 | 6,10 | 21,21 |

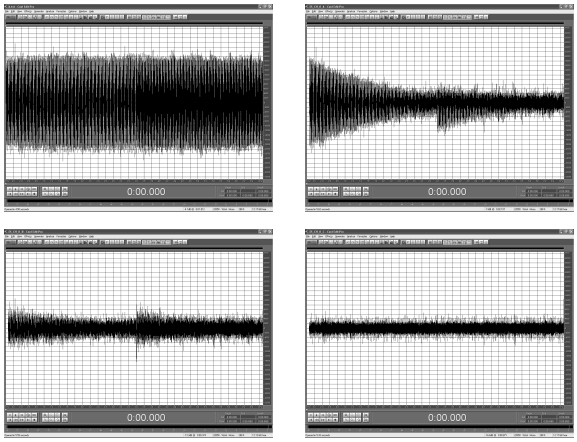


*Fig. 31. a-d. Test signal (top left, a). Error signals: Basic system (top right, b). Sinusoidal initial waveform (bottom left, c). Referent signal as initial waveform (bottom right, d).*

### 9.5 Incorporating cabin acoustics

In real implementation attenuation results would be somewhat lower because of sound reverberation in closed space) that distorts canceling sound from secondary sources and deforms canceling acoustic signal waveform at the point of desired noise cancellation. To assess the effectiveness of the system in real conditions acoustic measurements (impulse responses) have been performed for the purposes of its acoustic characterization. The impulse response is a transfer function between the signal source and the receiver. When it is measured in an aircraft cabin, it includes the information of sound reflection, absorption, and reverberation. Measurements were performed using the MLS (Maximum Length Sequence) and TSP (Time Stretched Pulse) method, (sample rate $44.1$ kHz). The simple characterization of the acoustic space was achieved with the help of a few impulse responses and attenuation factors between the source and the microphone when measuring the raw impulse response (because the measured values and normalized impulse response from them can determine the signal loss). Then, the respective values of the impulse responses are included in the algorithm that was previously developed and described. Measurements were carried out in the cockpit of the Cessna 172N. Three impulse responses have been measured. The sound source was placed behind the instrument panel and the microphone was moved across all seat positions at the head level. First measurement was with the sound source behind the windshield and measurement microphone at the position of pilot ear seating on the front seat (Fig. 32). Second impulse response has been measured with the sound source behind the windshield and measurement microphone at the position of pilot ear seating on the front seat (Fig. 33).

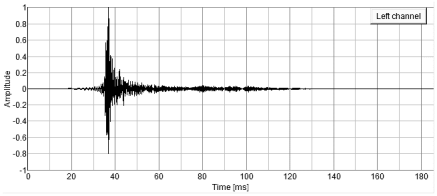


*Fig. 32. Impulse response - windshield – front seat passenger ear.*

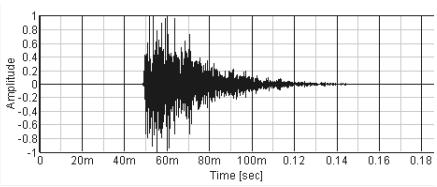


*Fig. 33. Impulse response – windshield – rear seat passenger ear.*

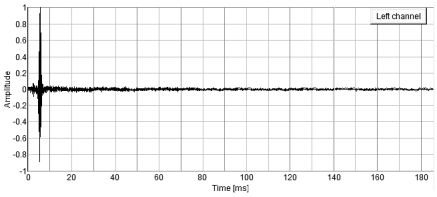


*Fig. 34. Impulse response –secondary source placed at the top of the cabin right above the head and ear.*

Third impulse response has been measured with the sound source at the cabin ceiling above the head (position of secondary source of ANC system) and measuring microphone at ear position of pilot on front seat (Fig. 34).

Measured impulse responses were used in auralization process to incorporate the cabin echo into the attenuation results, Fig. 35. The auralization filter I was applied to test signal that was measured (recorded) behind the windshield and the auralization filter II to the signal originating from the secondary (i.e. noise canceling) source. The simulation was performed with four noise test signals (same as in the single-channel system). The results are slightly poorer than those obtained by simulation with far greater simplification (a combination of weakening-delay without any impulse response). Achieved ANR attenuation results on front seat positions are presented in Tables 9-11.

Moderate but realistic noise attenuation values were achieved, comparable with other methods. Similar conservative values were achieved with some other experimental or low quantity production commercial systems.

Impact of the echo on the operation of the system can be summarized by the following points:

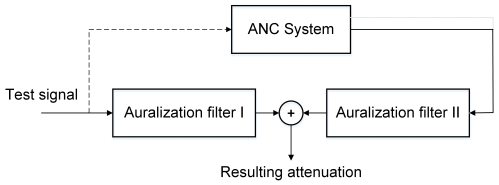


*Fig. 35. Auralization in noise attenuation simulation process.*

*Table 9. Noise attenuation for the basic system (auralization included)*

| Test signal | Attenuation with various weighting | | |
|---|---|---|---|
| | *unweigh.* | *A-weighting* | *C-weighting* |
| C172_rpm1 | 10,45 | -1,08 | 10,23 |
| C172_rpm2 | 11,27 | -2,24 | 10,68 |
| C172_rpm3 | 9,96 | -3,02 | 9,48 |
| C172_rpm4 | 16,54 | 0,32 | 16,25 |

1. There is notable degradation of noise reduction of about 2-6 dB depending on a particular case (degradation is higher at higher attenuations)

2. Convergence time increased (more than twice). In some cases even 6s of the test signal was not enough for achieving the full convergence. In those cases better results could be achieved with longer test signals

3. Passive treatment of cabin surfaces with absorptive material is of an advantage not only due to better passive noise reduction, but also due to better predispositions for operation of the ANC system. This is understandable because simplifying or eliminating echos simplifies the acoustic field in a cabin.

4. Sensitivity of the ANC system to the echoes within the cabin is partially related to the reflections of the secondary sources (distorting the desired noise cancelling signal) and partially due to the coherent averaging because echo last longer than the averaging period. Better results could possibly be achieved with the corrected secondary source signal that would incorporate the influences of longer reflections and then

*Table 10. Noise attenuation for the advanced system with sinusoidal preloading (auralization included)*

| Test signal | Attenuation with various weighting | | |
|---|---|---|---|
| | *unweigh.* | *A-weighting* | *C-weighting* |
| C172_rpm1 | 9,10 | -1,11 | 9,92 |
| C172_rpm2 | 11,57 | -2,32 | 10,92 |
| C172_rpm3 | 9,90 | -3,04 | 9,45 |
| C172_rpm4 | 16,70 | 0,30 | 16,44 |

*Table 11. Noise attenuation for the advanced system with referent signal preloading (auralization included)*

| Test signal | Attenuation with various weighting | | |
|---|---|---|---|
| | *unweigh.* | *A-weighting* | *C-weighting* |
| C172_rpm1 | 9,48 | -0,99 | 9,96 |
| C172_rpm2 | 10,85 | -2,06 | 10,33 |
| C172_rpm3 | 11,74 | -2,49 | 11,24 |
| C172_rpm4 | 17,74 | -0,74 | 17,53 |

coherent averaging of more periods (two, three), with the running averaging window with 1-2 period shift.

## 10 CONCLUSION

The method for active noise reduction using coherent averaging of residual signal is presented. New algorithm is presented which avoids use of a digital filter and the LMS adaptation. It is simple, intuitive and is not numerically intensive. The method is restricted to active control of periodic or nearly periodic noise that is most common in cabins of general aviation aircraft. Due to low numerical complexity method can be implemented in very cheap hardware, like conventional microcontrollers. Broadband noise originating from fuselage slipstream air must be addressed separately with conventional passive techniques. Moderate but realistic attenuation values have been achieved, comparable with other methods used in experimental and some rare commercial systems. There is a tradeoff between numerical complexity and necessity for calibration of ANC system before first use of the system. Determination of the time delay in acoustic path (including phase shift in loudspeaker) is accomplished by the calibration process using the short pilot tone before the first use of the device.

## REFERENCES

[1] D. Miljković, Active noise control in light aircraft cabin using multichannel coherent method, PhD thesis, University of Zagreb, Faculty of Electrical Engineering and Computing, 2006

[2] J. F. Unruh and P. D. Till, "General Aviation Interior Noise: Part I-III – Source/Path Identification Technology", tech. rep. NASA/CR-2002-21165, Southwest Research Inst., San Antonio, Texas, May 2002

[3] D. Miljković, "Comparative Investigation of Aircraft Interior Noise Properties", Proceedings of the 3rd Congress of the Alps Adria Acoustics Association, Graz, Austria, 27–28 September 2007

[4] D. Miljković, J. Ivošević and T. Bucak, "Two vs. Three Blade Propeller - Cockpit Noise Comparison", Proceedings of the 5th Congress of the Alps Adria Acoustics Association, Petrčane, Croatia, 12-14 September 2012

[5] D. Miljković, J. Ivošević, and T. Bucak, "Psycho-acoustical Ergonomics in a light Aircraft Interior", Proc. 5th International Ergonomics Conference, Zadar, Croatia, June 2013

[6] Newman J. S. and Beattie K. R., "Aviation Noise Effects", Report No. FAA-EE-85-2, US DoT FAA, March 1985

[7] L. R. Miller, D. J. Rossetti and M. A. Norris, "Passive, Active and Hybrid Solutions for Aircraft Interior Noise Problems", Tech. Rep. LL-6007, Lord Corporation, Nov. 1995

[8] D. Miljković, M. Maletić and B. Somek, "Active Noise Control", Proceedings of the MIPRO 2007, Opatija, Croatia, May 2007

[9] H. G. Leventhall and L. Wong, "A Review of Active Attenuation And Development of an Active Attenuator 'Open Refuge", HSE Contract Res. Rpt. No. 4/1988, WS Atkins Engin. Sciences, 1988

[10] S. M. Kuo and D. R. Morgan, "Active Noise Control: A Tutorial Review", Proceedings of the IEEE, Vol. 87, No. 6, June 1999

[11] T. Priede, "Noise and Vibration Control of the Internal Combustion Reciprocating Engine", in Noise and Vibration Engineering, pp. 665-708, John Wiley, 1992

[12] A. Barber, Handbook of Noise and Vibration Control, Elsevier, 1993

[13] G. J. J. Ruijgrok, Elements of aviation acoustics, Delft University Press, Delft, 1993

[14] B. Widrow and S. D. Stearns, Adaptive Signal Processing, Prentice Hall, 1985

[15] P. Tagare, Signal Averaging, Biomedical Digital Signal Processing (J. Tomkins, Ed.), Prentice Hall, 1993

[16] Cessna 172N Skyhawk, Pilot's Operating Handbook, Cessna, 1977

**D. Miljković** holds B.Sc., M.Sc. and Ph.D. degree from Faculty of Electrical Engineering and Computing, Zagreb, Croatia. He has spent 14 months specializing speech recognition at University of Cambridge, UK. At present he is with Hrvatska elektroprivreda (Croatian Electricity Company) working on highly available business systems. Dr. Miljković is author of over sixty scientific and professional papers. He is executive editor of CrSNDT Journal (Journal of Croatian Society of Non-Destructive Testing) and a member of IEEE, CrSNDT and AMAC.

## AUTHORS' ADDRESSES

**Dubravko Miljković, Ph.D.**
**Hrvatska elektroprivreda d.d.,**
**37 City of Vukovar Street, 10000 Zagreb,**
**email: dmiljkovic@hep.hr**

Received: 2016-02-22
Accepted: 2017-04-18